

# EFFECTIVE MACRODIFFUSION IN SOLUTE TRANSPORT THROUGH HETEROGENEOUS POROUS MEDIA

BRAHIM AMAZIANE\*, ALAIN BOURGEAT†, AND MLADEN JURAK‡

**Abstract.** Homogenization method is used to analyze the global behavior of passive solute transport through highly heterogeneous porous media. The flow is governed by a coupled system of an elliptic equation and a linear convection-diffusion concentration equation with a diffusion term small with respect to the convection, i.e. with a relatively high Peclet number. We use asymptotic expansions techniques in order to define a macroscale transport model. Numerical computations to obtain the effective hydraulic conductivity and the macrodiffusivity tensor are presented, using finite volume methods. Numerical experiments based on typical situations encountered in the simulations of solute transport have been performed comparing the transport in the heterogeneous medium to the transport in the corresponding effective medium. The results of the simulations are compared in terms of spatial moments,  $L^2$  errors and concentration contours. From all those points of view the results obtained from the simulations using the effective model obtained by the homogenization method show good agreement with the heterogeneous simulations.

**Key words.** dispersion, heterogeneous porous media, homogenization, solute transport

**AMS subject classifications.** 74Q15, 74S10, 76M50, 76R99, 76S05

**1. Introduction.** In a previous paper [12], we gave a mathematical model for explaining how the upscaling of a diffusive but dominant convective transport model at a mesoscale, in an aquifer with highly contrasted geology, may produce a global model including, at a macroscale, convection enhanced effective diffusivity tensors. For this it was necessary to make precise assumption on the Darcy's velocity at the aquifer scale, or equivalently on the Peclet number, assuming it was of order  $1/\varepsilon$ , where  $\varepsilon$  is a small parameter. The goal of the present paper is to present numerical simulations based on periodic homogenization to prove numerically the accuracy of our mathematical modeling and to compare to classical models used in geohydrology literature like for instance [6], [10], [20], [35], [19], [37]. For this, we are comparing numerical simulations of typical situations of flow and transport through heterogeneous porous media where mechanical dispersion could appear. The understanding and prediction of fluid flow through porous media is of great importance in various areas of research and industry. Petroleum engineers need to model multiphase and multicomponent flow for production of hydrocarbons from petroleum reservoirs. Hydrologists and soil scientists are concerned with underground water flow in connection with applications to civil and agricultural engineering, and, of course, the design and evaluation of remediation technologies in water quality control rely on the properties of underground fluid flow. More recently, modeling flow and transport of contaminant received an increasing attention in connection with the behavior of an underground repository of radioactive waste (see, e. g., [13]).

The physical situation we address here corresponds to the transport of solute in a highly heterogeneous aquifer by groundwater flow due to the hydraulic head and by diffusion coming from the dilution of the solute in the water. The governing equa-

---

\*Laboratoire de Mathématiques Appliquées, CNRS-UMR5142, Université de Pau, av. de l'Université, 64000 Pau, France, ([brahim.amaziane@univ-pau.fr](mailto:brahim.amaziane@univ-pau.fr)).

†Université Lyon I - ISTIL, Equipe MCS, 15 bld. Lataret, 69622 Villeurbanne Cedex, France, ([bourgeat@mcs.univ-lyon1.fr](mailto:bourgeat@mcs.univ-lyon1.fr)).

‡Department of Mathematics, University of Zagreb, Bijenička c. 30, 10000, Zagreb, Croatia, ([jurak@math.hr](mailto:jurak@math.hr)).

tions arise from the laws of conservation of mass of the fluid, along with a constitutive relation relating the fluid velocity which appears in the conservation law to the hydraulic head. Traditionally, the standard Darcy equation provides this relation. This process can be formulated as a coupled system of partial differential equations which includes an elliptic hydraulic head-velocity equation and a linear convection-diffusion concentration equation, subject to appropriate boundary and initial conditions.

It is known that periodicity could be seen as an example of stationary random field, see [25], [34], and we assume periodicity of the heterogeneities in order to simplify both the mathematical derivation of the macroscopic model and the computation of the macroscopic hydrogeological parameters. In fact, with classical stochastic assumption, the computation of local problems have to be done on a sufficiently large representative elementary volume R.E.V. instead of a single periodic cell, and instead of usual asymptotic expansion we should use either two-scale convergence for partial differential equations in probability space like in [14] or convergence of process solution of a stochastic differential equation like in [17]. However as seen in [23] the results with random flows could be different from periodic flows.

The outline of the remainder of the paper is as follows. In Section 2 we give a short description of the mathematical and physical model used in this study and the main assumptions. In Section 3 and Section 4, the homogenization method is briefly presented by recalling the mesoscale and the macroscale equations with the local problems. Starting from the heterogeneity geometry and from the spatial localization of these heterogeneities we show how to compute the corresponding convection enhanced effective diffusivity tensor and the effective hydraulic conductivity for different heterogeneity shapes and different hydrogeological properties. Finally focusing on one shape of heterogeneity, we derive the corresponding effective macroscopic model including the effects of mechanical dispersion in its effective macrodiffusivity tensor for two different flow regime. The determination of the effective hydraulic conductivity requires numerical approximation of elliptic equations solutions in a periodic cell. To compute the effective macrodiffusivity tensor we have to solve local convection-diffusion problems in a periodic cell. We use a finite volume method to solve these local problems and to compute both the effective hydraulic conductivity and the effective macrodiffusivity tensor. In Section 4 we discuss the importance of different symmetries for the heterogeneities in the aquifer and show how they modify the calculation of the effective hydrogeological properties. Sections 5 and 6 are devoted to the presentation of the numerical simulations and we illustrate the performance of our upscaling by presenting two cases derived from typical 2D examples of pollutant spreading in an aquifer, like in [6]. We simulate the transport of a solute in a porous domain using both the mesoscopic model and the macroscopic dispersive model, and we compare the heterogeneous and homogeneous scaled up results by computing the corresponding spatial moments, the  $L^2$  errors and concentration contours.

**2. Formulation of the problem.** The miscible displacement of an incompressible fluid with a dissolved solute in a heterogeneous confined aquifer  $\Omega \subset \mathbb{R}^d$   $d = 1, 2, 3$  over a time period  $(0, T)$ , is given by (see, e.g., [10]):

$$\phi(x) \frac{\partial c}{\partial t} + \vec{q}(x) \cdot \nabla c = \operatorname{div}(\mathbb{D}(x) \nabla c) \quad \text{in } \Omega \times (0, T), \quad (2.1)$$

where  $\vec{q}(x)$  is the Darcy velocity, given by the hydraulic gradient  $\nabla H$ :

$$\vec{q} = -\mathbb{K} \nabla H, \quad \operatorname{div} \vec{q} = 0 \quad \text{in } \Omega, \quad (2.2)$$

subject to appropriate boundary and initial conditions. Here  $c(x, t)$  is the transported solute concentration,  $\phi$  and  $\mathbb{K}$  are the porosity and the hydraulic conductivity tensor of the heterogeneous medium, and  $\mathbb{D}$  is the diffusivity tensor at the Darcy scale.

We assume, as explained in the introduction, that the heterogeneous porous medium in the aquifer has a network of uniformly spaced heterogeneities with a block size  $l$  which is small compared to the size  $L$  of the aquifer. Namely, we assume the separation of scales, which can be expressed as  $0 < l \ll L$ . First we express this local description (2.1)-(2.2) in a dimensionless form and we analyze the orders of magnitude of the dimensionless parameters appearing in this new formulation. The dimensionless equations are obtained by introducing dimensionless variables from any physical variable. For this, denoting  $q^0$ ,  $D^0$ ,  $K^0$  and  $\phi^0$  the characteristic Darcy's velocity, diffusivity, permeability and rock porosity, we define  $\varepsilon = l/L$ ,  $\text{Pe} = q^0 l/D^0$  and  $\tau_c = \phi^0 L/q^0$ .

Assuming moreover that the porosity, the hydraulic conductivity tensor, and the diffusivity tensor in the heterogeneous medium are rapidly oscillating functions depending on  $y = x/\varepsilon$ , the mesoscale, we introduce in (2.1)–(2.2) the dimensionless space variable  $x \mapsto x/L$  and the dimensionless characteristic convection time  $t \mapsto t/\tau_c$ . We obtain finally the dimensionless governing system of equations:

$$\phi\left(\frac{x}{\varepsilon}\right) \frac{\partial c^\varepsilon}{\partial t} + \vec{q}^\varepsilon(x) \cdot \nabla c^\varepsilon = \frac{\varepsilon}{\text{Pe}} \text{div}\left(\mathbb{D}\left(\frac{x}{\varepsilon}\right) \nabla c^\varepsilon\right) \quad \text{in } \Omega \times (0, T), \quad (2.3)$$

$$\vec{q}^\varepsilon = -\mathbb{K}\left(\frac{x}{\varepsilon}\right) \nabla H^\varepsilon, \quad \text{div} \vec{q}^\varepsilon = 0 \quad \text{in } \Omega. \quad (2.4)$$

In the above equations (2.3)-(2.4), although all the quantities are now dimensionless, we have kept the same notations as before in (2.1)–(2.2).

The constant number  $\text{Pe}$ , the local Peclet number, represents the convection diffusion ratio at the heterogeneities scale (mesoscale). As usual for homogenization of convection-diffusion problems (see for instance [38], [32], [25]), our two main assumptions are the separation of scales,  $0 < \varepsilon \ll 1$  and  $\text{Pe} = O(1)$ . The dimensionless parameters  $\phi$ ,  $\mathbb{D}$  and  $\mathbb{K}$  in (2.3)-(2.4) are assumed to be  $Y$ -periodic functions, where the periodicity cell is  $Y = (0, l_1) \times \cdots \times (0, l_d)$ , and the domain  $\Omega$  and the time  $T$ , are rescaled dimensionless domain and time.

Using formal multiscales asymptotic expansions of (2.3)-(2.4), we could derive the macroscopic behavior of the system (see, for instance, [8], [33], [12]). In [12], the boundary layers correctors were constructed for Dirichlet boundary conditions in an infinite strip, and the convergence of the expansion, at any order, was rigorously justified.

Throughout the paper we will use the convention of summation over repeated indices.

**3. Asymptotic analysis of the model.** In this Section we recall the notations and the main results of [12], and for simplicity, we will proceed with the expansion, up to the second order, in the interior of the domain, but neglecting the boundary layers influence.

**3.1. Asymptotic expansion for the Darcy law.** The method and convergence results for the asymptotic expansion at any order of the Darcy velocity, including the boundary layer correctors, were presented in details in Section 3 of [12], and here we present only the first two terms in the asymptotic expansion of the Darcy velocity, without any boundary layer correctors. All these results are standard and we

will only write the results and notations necessary for understanding the next section. We start by defining the hydraulic head (or pressure) expansion:

$$H^\varepsilon(x) \approx \overline{H}^0(x) + \varepsilon H^1(x, \frac{x}{\varepsilon}) + \varepsilon^2 H^2(x, \frac{x}{\varepsilon}) + \dots \quad (3.1)$$

$$H^1(x, y) = \chi_i^1(y) \partial_i \overline{H}^0(x) + \overline{H}^1(x), \quad (3.2)$$

$$H^2(x, y) = \chi_{i,j}^2(y) \partial_{i,j}^2 \overline{H}^0(x) + \chi_i^1(y) \partial_i \overline{H}^1(x) + \overline{H}^2(x).$$

Then the Darcy velocity  $\vec{q}^\varepsilon$  in (2.4), is approximated by:

$$\vec{q}^\varepsilon(x) \approx \vec{Q}^0(x, x/\varepsilon) + \varepsilon \vec{Q}^1(x, x/\varepsilon) + \dots$$

with

$$\begin{aligned} \vec{Q}^0(x, y) &= -\mathbb{K}(y) (\nabla_y \chi_i^1(y) + \vec{e}_i) \partial_i \overline{H}^0(x), \\ \vec{Q}^1(x, y) &= -\mathbb{K}(y) \left[ (\nabla_y \chi_{i,j}^2(y) + \chi_i^1(y) \vec{e}_j) \partial_{i,j}^2 \overline{H}^0(x) + (\nabla_y \chi_i^1(y) + \vec{e}_i) \partial_i \overline{H}^1(x) \right], \end{aligned}$$

where  $(\vec{e}_i)_{1 \leq i \leq d}$  is the standard basis of  $\mathbb{R}^d$ . The functions  $\chi_i^1$  and  $\chi_{i,j}^2$  are  $Y$ -periodic and defined by the two following sequences of local problems defined in  $Y$ :

$$\operatorname{div}_y (\mathbb{K}(y) (\nabla_y \chi_i^1 + \vec{e}_i)) = 0 \quad \text{in } Y, \quad (3.3)$$

for  $i = 1, \dots, d$  and

$$\begin{aligned} -\operatorname{div}_y (\mathbb{K} (\nabla_y \chi_{i,j}^2 + \vec{e}_j \chi_i^1)) \\ = (\mathbb{K} (\nabla_y \chi_i^1 + \vec{e}_i) - \langle \mathbb{K} (\nabla_y \chi_i^1 + \vec{e}_i) \rangle) \cdot \vec{e}_j \quad \text{in } Y, \end{aligned} \quad (3.4)$$

for  $i, j = 1, \dots, d$ .

We use in (3.4), and through out the paper, the standard notation  $\langle \cdot \rangle$  for the mean value over the periodic cell  $Y$ . From the vectors

$$\vec{w}^i(y) = -\mathbb{K}(y) (\nabla_y \chi_i^1(y) + \vec{e}_i), \quad i = 1, \dots, d$$

we build the matrix

$$\mathbb{Q}(y) = [\vec{w}^1(y), \dots, \vec{w}^d(y)], \quad (3.5)$$

and we define the *effective hydraulic conductivity*

$$\mathbb{K}^h = -\langle \mathbb{Q} \rangle = -\frac{1}{|Y|} \int_Y \mathbb{Q}(y) dy. \quad (3.6)$$

Then, the first term in the expansion of  $\vec{q}^\varepsilon$  is now:

$$\vec{Q}^0(x, y) = \mathbb{Q}(y) \nabla \overline{H}^0(x), \quad \text{with } \operatorname{div} (\mathbb{K}^h \nabla \overline{H}^0) = 0 \quad \text{in } \Omega. \quad (3.7)$$

Similarly, to compute the second term in the hydraulic head expansion, we should solve the problem

$$-\operatorname{div}(\mathbb{K}^h \nabla \overline{H}^1) = \operatorname{div} \left( \sum_{i,j=1}^2 \mathbf{N}_{i,j}^2 \partial_i \partial_j \overline{H}^0 \right) \quad \text{in } \Omega; \quad (3.8)$$

where

$$\mathbf{N}_{i,j}^2 = \langle \mathbb{K}(\nabla_y \chi_{i,j}^2 + \chi_i^1 \vec{e}_j) \rangle. \quad (3.9)$$

But using variational formulation of the problem (3.4) we remark that:

$$\vec{\mathbf{N}}_{i,j}^2 \cdot \vec{e}_l = \langle \mathbb{K}(\nabla \chi_l^1 + \vec{e}_l) \chi_i^1 - \mathbb{K}(\nabla \chi_i^1 + \vec{e}_i) \chi_l^1 \rangle \cdot \vec{e}_j; \quad (3.10)$$

namely, the vectors  $\vec{\mathbf{N}}_{i,j}^2$  are *skew-symmetric*:  $\vec{\mathbf{N}}_{i,j}^2 \cdot \vec{e}_l = 0$  for  $i = l$ , and  $\vec{\mathbf{N}}_{i,j}^2 \cdot \vec{e}_l = -\vec{\mathbf{N}}_{l,j}^2 \cdot \vec{e}_i$  for  $i \neq l$ . With this last property, equation (3.8) reduces then to

$$\operatorname{div}(\mathbb{K}^h \nabla \overline{H}^1) = 0 \quad \text{in } \Omega. \quad (3.11)$$

**REMARK 3.1.** In (3.1) we impose the first term  $\overline{H}^0$  to satisfy the same boundary conditions as the heterogeneous head  $H^\varepsilon$ . In order to correct oscillations on the boundary produced by the following periodic terms in the expansion (3.1), boundary layer correctors should be added. For this, in [12] Section 3, we split each  $\chi^1$  and  $\chi^2$  in a  $Y$ -periodic term  $\chi^{k,\#}$  and two boundary layer corrector terms  $\chi^{k,\pm}$ . But, in turn, these boundary layer correctors produce a small error, of order  $\varepsilon$ , in the whole domain which is then corrected at the next order by introducing the term  $\overline{H}^1$ . Since we consider herein a simplified expansion without considering the boundary layers, we will have  $\overline{H}^1 = 0$  in (3.2).

Finally, discarding boundary layers and oscillating higher order terms, we approximate  $\vec{q}^\varepsilon$  by:

$$\vec{q}^\varepsilon(x) \approx \vec{q}^0(x) + \varepsilon \vec{q}^1(x), \quad (3.12)$$

with

$$\vec{q}^0 = \langle \vec{Q}^0 \rangle = -\mathbb{K}^h \nabla \overline{H}^0, \quad \vec{q}^1 = \langle \vec{Q}^1 \rangle = -\vec{\mathbf{N}}_{i,j}^2 \partial_{i,j}^2 \overline{H}^0. \quad (3.13)$$

**3.2. Asymptotic expansion for the concentration.** Like for the hydraulic head, we seek an asymptotic expansion for the concentration equation in the interior of the domain, outside the boundary layers, in the form:

$$c^\varepsilon(x, t) \approx c^0(x, x/\varepsilon, t) + \varepsilon c^1(x, x/\varepsilon, t) + \dots. \quad (3.14)$$

First, the term,  $c^0 = \overline{c}^0(x, t)$  is a solution of the first order hyperbolic equation

$$\langle \phi \rangle \frac{\partial \overline{c}^0}{\partial t} + \langle \vec{Q}^0 \rangle \cdot \nabla_x \overline{c}^0 = 0 \quad \text{in } \Omega \times (0, T), \quad (3.15)$$

and the second one,  $c^1$  has the form

$$c^1 = \psi_k(x, y) \frac{\partial \overline{c}^0}{\partial x_k}(x, t) + \overline{c}^1(x, t). \quad (3.16)$$

In (3.16)  $\psi_k(x, \cdot)$  is a  $Y$ -periodic solution of the local problem:

$$-\frac{1}{\text{Pe}} \text{div}_y (\mathbb{D}(y)(\nabla_y \psi_k + \vec{e}_k)) + \vec{Q}^0 \cdot \nabla_y \psi_k = \left[ \frac{\phi(y)}{\langle \phi \rangle} \langle \vec{Q}^0 \rangle - \vec{Q}^0 \right] \cdot \vec{e}_k \quad \text{in } Y, \quad (3.17)$$

and  $\bar{c}^1$  is a solution of:

$$\langle \phi \rangle \frac{\partial \bar{c}^1}{\partial t} + \langle \vec{Q}^0 \rangle \cdot \nabla \bar{c}^1 + \langle \vec{Q}^1 \rangle \cdot \nabla \bar{c}^0 = \frac{1}{\text{Pe}} \text{div}(\mathbb{D}_*^h(x) \nabla \bar{c}^0) \quad \text{in } \Omega \times (0, T), \quad (3.18)$$

with

$$\mathbb{D}_*^h(x) \vec{e}_k = \langle \mathbb{D}(\nabla_y \psi_k + \vec{e}_k) \rangle + \text{Pe} \langle \left( \frac{\phi(y)}{\langle \phi \rangle} \langle \vec{Q}^0 \rangle - \vec{Q}^0 \right) \psi_k \rangle. \quad (3.19)$$

**Definition of the macroscale concentration**  $c^{1,\varepsilon}(x, t)$ :

Following Section 6 in [12] we define a *macroscale concentration*,  $c^{1,\varepsilon}(x, t)$ , from the non-oscillatory terms in the expansion (3.14); precisely, we denote

$$c^{1,\varepsilon}(x, t) = \bar{c}^0(x, t) + \varepsilon \bar{c}^1(x, t).$$

Summing up, equations (3.15) and (3.18), leads to the equation satisfied by  $c^{1,\varepsilon}(x, t)$ :

$$\langle \phi \rangle \frac{\partial c^{1,\varepsilon}}{\partial t} + \bar{q}^0 \cdot \nabla_x c^{1,\varepsilon} + \varepsilon \bar{q}^1 \cdot \nabla_x \bar{c}^0 = \frac{\varepsilon}{\text{Pe}} \text{div}_x (\mathbb{D}_*^h(x) \nabla_x \bar{c}^0) \quad \text{in } \Omega \times (0, T),$$

and we conclude (see for details Section 6 in [12]) that the macroscale concentration obey, with precision  $O(\varepsilon^2)$ , the effective macroscale equation:

$$\langle \phi \rangle \frac{\partial c^{1,\varepsilon}}{\partial t} + (\bar{q}^0 + \varepsilon \bar{q}^1) \cdot \nabla_x c^{1,\varepsilon} = \frac{\varepsilon}{\text{Pe}} \text{div}_x (\mathbb{D}_*^h(x) \nabla_x c^{1,\varepsilon}) \quad \text{in } \Omega \times (0, T). \quad (3.20)$$

It is interesting to notice that equation (3.20) could be seen as a viscous approximation of the first order hyperbolic equation (3.15).

**Definition of the effective macrodiffusivity tensor**  $\mathbb{D}^h$ :

The macroscopic effective hydraulic conductivity  $\mathbb{K}^h$  is obtained by standard homogenization procedure as recalled in (3.3), (3.5) and (3.6). The determination of  $\mathbb{K}^h$  requires the numerical approximation of the solution of  $d$  elliptic equations (3.3) in the periodic cell  $Y$ .

According to (3.5)-(3.7) and (3.17), in order to compute the effective macrodiffusivity  $\mathbb{D}_*^h$  we have first to find the  $Y$ -periodic solutions  $y \mapsto \psi_k(y; \vec{\lambda})$  of the  $d$  convection-diffusion equations:

$$-\text{div}_y (\mathbb{D}(y)(\nabla_y \psi_k + \vec{e}_k)) + \mathbb{Q}(y) \vec{\lambda} \cdot \nabla_y \psi_k = \left[ \frac{\phi(y)}{\langle \phi \rangle} \langle \mathbb{Q} \rangle \vec{\lambda} - \mathbb{Q}(y) \vec{\lambda} \right] \cdot \vec{e}_k \quad \text{in } Y, \quad (3.21)$$

$k = 1, \dots, d$ , for every  $\vec{\lambda} = \text{Pe} \nabla \bar{H}^0(x)$ , and secondly to compute, according to (3.19), the tensor

$$\mathcal{D}^h(\vec{\lambda}) \vec{e}_k = \langle \mathbb{D}(\nabla_y \psi_k + \vec{e}_k) \rangle + \langle \left( \frac{\phi(y)}{\langle \phi \rangle} \langle \mathbb{Q} \rangle \vec{\lambda} - \mathbb{Q} \vec{\lambda} \right) \psi_k \rangle, \quad (3.22)$$

and then we have  $\mathbb{D}_*^h(x) = \mathcal{D}^h(\text{Pe} \nabla \bar{H}^0(x))$ . To this tensor we will add a skew-symmetric part coming from the convective term as follows. The first order correction  $\bar{q}^1 = \langle \vec{Q}^1 \rangle$  to the effective Darcy's velocity  $\bar{q}^0 = \langle \vec{Q}^0 \rangle$  is given by (3.13), and using the *skew-symmetry* of the vectors  $\vec{N}_{i,j}^2$  (see (3.10)), we denote in (3.20)

$$-\bar{q}^1 \cdot \nabla c^{1,\varepsilon} = \vec{N}_{i,j}^2 \partial_{i,j}^2 \bar{H}^0 \cdot \nabla c^{1,\varepsilon} = \text{div}(\mathcal{M}(\nabla \bar{H}^0) \nabla c^{1,\varepsilon}), \quad (3.23)$$

with the skew-symmetric matrix  $\mathcal{M}(\nabla\overline{H}^0)$  given by

$$\mathcal{M}(\nabla\overline{H}^0)_{i,l} = (\vec{\mathbf{N}}_{i,j}^2 \cdot \vec{e}_l) \partial_j \overline{H}^0. \quad (3.24)$$

Finally, taking into account (3.23), we obtain the complete *effective macrodiffusivity*

$$\mathbb{D}^h(x) = \mathcal{D}^h(\text{Pe}\nabla\overline{H}^0(x)) + \mathcal{M}(\text{Pe}\nabla\overline{H}^0(x)), \quad (3.25)$$

and we can write the dimensionless *effective macroscale equations* in the form:

$$\langle \phi \rangle \frac{\partial c^{1,\varepsilon}}{\partial t} + \vec{q}^0 \cdot \nabla_x c^{1,\varepsilon} = \frac{\varepsilon}{\text{Pe}} \text{div}_x (\mathbb{D}^h(x) \nabla_x c^{1,\varepsilon}) \quad \text{in } \Omega \times (0, T), \quad (3.26)$$

$$\vec{q}^0 = -\mathbb{K}^h \nabla \overline{H}^0, \quad \text{div} \vec{q}^0 = 0 \quad \text{in } \Omega. \quad (3.27)$$

REMARK 3.2. Note that  $\psi_k(y; \vec{\lambda})$  depends on the global variable  $x$  through the vector  $\vec{\lambda} = \text{Pe}\nabla\overline{H}^0(x)$  and moreover the dependence on  $\vec{\lambda}$  is nonlinear.

Although  $\mathbb{D}^h(x)$  is not symmetric in general, it is not difficult to show that it is positive definite, and therefore problem (3.26), (3.27), with suitable boundary conditions, is well posed. Namely, from the variational formulation of equation (3.21), for any  $\vec{\xi} \in \mathbb{R}^d$ , it follows

$$\mathcal{D}^h(\vec{\lambda}) \vec{\xi} \cdot \vec{\xi} = \langle \mathbb{D}(\nabla_y \psi_{\vec{\xi}} + \vec{\xi}) \cdot (\nabla_y \psi_{\vec{\xi}} + \vec{\xi}) \rangle, \quad (3.28)$$

where  $\psi_{\vec{\xi}} = \xi_k \psi_k$ . Since  $\psi_{\vec{\xi}}$  is a periodic function, the right hand side is strictly positive for all  $\vec{\xi} \neq 0$ .

REMARK 3.3. From physical point of view problems (3.21) represent a simplified model of small scale fluctuations in the concentration  $c^\varepsilon$ , induced by the small scale fluctuations in the Darcy velocity. These fluctuations have a dispersive effect on solute particles, which can be much stronger than dispersion due to molecular diffusion, and which is usually called **mechanical dispersion**. The effective macroscale model (3.26), (3.27) takes the mechanical dispersion into account through the effective macrodiffusivity tensor  $\mathbb{D}^h$ , using the small scale fluctuation model (3.21). If we take, for simplicity, a constant and isotropic  $\mathbb{D} = d\mathbb{I}$ , then from (3.28) we have  $\mathcal{D}^h(\vec{\lambda})_{i,i} = d(1 + \langle |\nabla_y \psi_i|^2 \rangle)$ , which shows that our effective macrodiffusivity  $\mathbb{D}^h$  corresponds to a convection enhanced diffusion like in [25] or [22].

TO BE REMOVED It is easy to see, as for instance when  $\mathbb{D}$  is constant and diagonal, after developing formula (3.28) that our effective macrodiffusivity  $\mathbb{D}^h$  corresponds to a convection enhanced diffusion like in [25] or [22].

**4. Material symmetries.** In general, the effective macrodiffusivity tensor (3.25) is not symmetric; it also contains the skew symmetric term  $\mathcal{M}(\text{Pe}\nabla\overline{H}^0(x))$  coming from the convective part. Inspired by [26] and [22], we will show that with suitable symmetry of the aquifer heterogeneities the additional skew symmetric term in (3.25) disappears and the effective macrodiffusivity tensor becomes symmetric.

Let us consider a group of orthogonal matrices that preserve our periodicity lattice. For simplicity we consider only the reflections with respect to the coordinate axes and we denote  $\mathbf{C}_i = \text{diag}(1, \dots, -1, \dots, 1)$ , the diagonal matrix that has -1 in  $i$ -th row, and all other diagonal entries equal to 1, with  $\mathbf{C}_i^T$  denoting the transpose of the matrix  $\mathbf{C}_i$ .

Firstly, we formulate some well known results (see, e.g., [25]) concerning the periodic solutions  $\chi_i^1 \in H_{\#}^1(Y)$  of the problem (3.3), where  $H_{\#}^1(Y)$  is the space of the  $Y$ -periodic functions of  $H^1(Y)$ . Below we will use the uniqueness of the solutions of the cell problems, and for this we have normalized them by requiring the mean value to be equal to zero.

PROPOSITION 4.1. *Assume that for some  $i \in \{1, \dots, d\}$*

$$\forall z \in \mathbb{R}^d, \quad C_i^T \mathbb{K}(C_i z) C_i = \mathbb{K}(z). \quad (4.1)$$

Then for all  $z \in \mathbb{R}^d$  it holds

$$\begin{aligned} \chi_i^1(C_i z) &= -\chi_i^1(z), \quad \chi_j^1(C_i z) = \chi_j^1(z), \text{ for } j \neq i \\ \mathbb{Q}(C_i z) &= C_i \mathbb{Q}(z) C_i^T, \quad \mathbb{K}^h = C_i \mathbb{K}^h C_i^T, \end{aligned}$$

where the matrix  $\mathbb{Q}$  is given by (3.5), and  $\mathbb{K}^h$  by (3.6).

*Proof.* By simple change of variables  $y = C_i z$ , change of function  $v(z) = \chi_j^1(C_i z)$ , and orthogonality of the matrix  $C_i$ , we find

$$\operatorname{div}_y(\mathbb{K}(\nabla_y \chi_j^1 + \vec{e}_j))(C_i z) = \operatorname{div}_z(C_i^T \mathbb{K}(C_i z) C_i (\nabla_z v(z) + C_i^T \vec{e}_j)).$$

Since  $\langle v \rangle = \langle \chi_j^1 \rangle = 0$ , from the uniqueness of the solution of (3.3) we have  $v(z) = \chi_j^1(z)$  for  $j \neq i$  and  $v(z) = -\chi_i^1(z)$  for  $j = i$ . Other formulas follow from (3.5) and (3.6).  $\square$

PROPOSITION 4.2. *Let  $\mathbb{K}$  be diagonal and let (4.1) be satisfied for all  $i \in \{1, \dots, d\}$ . Then*

$$\vec{\mathbb{N}}_{i,j}^2 = 0 \quad \text{for all } i, j \in \{1, \dots, d\}.$$

*Proof.* If we assume that the tensor  $\mathbb{K}(y)$  is diagonal and that (4.1) is fulfilled for indices  $i$  and  $l$ , then from Proposition 4.1 we have

$$\langle \mathbb{K}(\nabla \chi_l^1 + \vec{e}_l) \chi_l^1 \rangle = \langle \mathbb{K}(\nabla \chi_i^1 + \vec{e}_i) \chi_l^1 \rangle = 0,$$

and therefore from (3.10)  $\vec{\mathbb{N}}_{i,j}^2 \cdot \vec{e}_l = 0$ , for all  $j$ .  $\square$

It is clear now that under the assumptions of Proposition 4.2, from (3.24) we have  $\mathcal{M}(\operatorname{Pe} \nabla \overline{H}^0(x)) = 0$ .

We now turn to the symmetry properties of the solution  $\psi_k \in H_{\#}^1(Y)$  of the problem (3.21), and the effective macrodiffusivity tensor  $\mathcal{D}^h(\vec{\lambda})$ , given by (3.22).

PROPOSITION 4.3. *For all  $\vec{\lambda} \in \mathbb{R}^d$  it holds  $\mathcal{D}^h(-\vec{\lambda}) = \mathcal{D}^h(\vec{\lambda})^T$ .*

*Proof.* Following [26], we denote by  $\psi_i \in H_{\#}^1(Y)$  the solution of equation (3.21), corresponding to a vector  $\vec{\lambda}$ , and  $\tilde{\psi}_i \in H_{\#}^1(Y)$  the solution corresponding to  $-\vec{\lambda}$ . Then using the variational formulation of (3.21), and taking two different indices  $i, j$  we get

$$\langle \mathbb{D}(\nabla \psi_i + \vec{e}_i) \cdot \nabla \tilde{\psi}_j \rangle + \langle \mathbb{Q} \vec{\lambda} \cdot \nabla \psi_i \tilde{\psi}_j \rangle = \frac{\langle \phi \tilde{\psi}_j \rangle}{\langle \phi \rangle} \langle \mathbb{Q} \vec{\lambda} \cdot \vec{e}_i \rangle - \langle \mathbb{Q} \vec{\lambda} \tilde{\psi}_j \rangle \cdot \vec{e}_i$$

and

$$\langle \mathbb{D}(\nabla \tilde{\psi}_j + \vec{e}_j) \cdot \nabla \psi_i \rangle - \langle \mathbb{Q} \vec{\lambda} \cdot \nabla \tilde{\psi}_j \psi_i \rangle = -\frac{\langle \phi \psi_i \rangle}{\langle \phi \rangle} \langle \mathbb{Q} \vec{\lambda} \cdot \vec{e}_j \rangle + \langle \mathbb{Q} \vec{\lambda} \psi_i \rangle \cdot \vec{e}_j.$$



From  $\operatorname{div}(\mathbb{Q}\vec{\lambda}) = 0$  it follows  $\langle \mathbb{Q}\vec{\lambda} \cdot \nabla \psi_i \tilde{\psi}_j \rangle = -\langle \mathbb{Q}\vec{\lambda} \cdot \nabla \tilde{\psi}_j \psi_i \rangle$ , and using the symmetry of the matrix  $\mathbb{D}$ , the two previous equations lead to

$$\begin{aligned} \langle \mathbb{D}(\nabla \psi_i + \vec{e}_i) \cdot \vec{e}_j + \frac{\langle \phi \tilde{\psi}_j \rangle}{\langle \phi \rangle} \langle \mathbb{Q} \vec{\lambda} \cdot \vec{e}_i - \langle \mathbb{Q} \vec{\lambda} \tilde{\psi}_j \rangle \cdot \vec{e}_i \rangle \\ = \langle \mathbb{D}(\nabla \tilde{\psi}_j + \vec{e}_j) \cdot \vec{e}_i - \frac{\langle \phi \psi_i \rangle}{\langle \phi \rangle} \langle \mathbb{Q} \vec{\lambda} \cdot \vec{e}_j + \langle \mathbb{Q} \vec{\lambda} \psi_i \rangle \cdot \vec{e}_j \rangle, \end{aligned}$$

which is exactly  $\mathcal{D}^h(\vec{\lambda})_{j,i} = \mathcal{D}^h(-\vec{\lambda})_{i,j}$ .  $\square$

PROPOSITION 4.4. *Assume that for some  $i \in \{1, \dots, d\}$*

$$\forall z \in \mathbb{R}^d, \quad C_i^T \mathbb{K}(C_i z) C_i = \mathbb{K}(z), \quad C_i^T \mathbb{D}(C_i z) C_i = \mathbb{D}(z), \quad \phi(C_i z) = \phi(z). \quad (4.2)$$

Then for all  $z \in \mathbb{R}^d$  it holds

$$\psi_i(C_i z; \vec{\lambda}) = -\psi_i(z; C_i^T \vec{\lambda}), \quad \psi_j(C_i z; \vec{\lambda}) = \psi_j(z; C_i^T \vec{\lambda}), \quad \text{for } j \neq i, \quad (4.3)$$

$$\mathcal{D}^h(\vec{\lambda}) = C_i \mathcal{D}^h(C_i^T \vec{\lambda}) C_i^T. \quad (4.4)$$

Moreover if (4.2) holds for all  $i \in \{1, \dots, d\}$ , then

$$\mathcal{D}^h(-\vec{\lambda}) = \mathcal{D}^h(\vec{\lambda}) = \mathcal{D}^h(\vec{\lambda})^T. \quad (4.5)$$

*Proof.* We introduce a  $Y$ -periodic function  $v(z; \vec{\lambda}) = \psi_j(C_i z; \vec{\lambda})$ , then by the change of variables  $y = C_i z$ , using Proposition 4.1 and (4.2) we get:

$$\begin{aligned} -\operatorname{div}_z (\mathbb{D}(z)(\nabla_z v(z) + C_i^T \vec{e}_j)) + \mathbb{Q}(z) C_i^T \vec{\lambda} \cdot \nabla_z v(z) \\ = \left[ \frac{\phi(z)}{\langle \phi \rangle} \langle \mathbb{Q} \rangle C_i^T \vec{\lambda} - \mathbb{Q}(z) C_i^T \vec{\lambda} \right] \cdot C_i^T \vec{e}_j. \end{aligned}$$

By the uniqueness of the solution we obtain (4.3).

To prove (4.4) we use the change of variables  $y = C_i z$  in the integrals over the periodic cell  $Y$ . By (4.3), (4.2) and Proposition 4.1 we get

$$\langle \mathbb{D}(\nabla \psi_j(\cdot; \vec{\lambda}) + \vec{e}_j) \rangle = C_i \langle \mathbb{D}(\nabla \psi_j(\cdot; C_i^T \vec{\lambda}) + \vec{e}_j) \rangle, \quad \text{for } j \neq i,$$

$$\langle \psi_j(\cdot; \vec{\lambda}) \mathbb{Q} \vec{\lambda} \rangle = C_i \langle \psi_j(\cdot; C_i^T \vec{\lambda}) \mathbb{Q} \rangle C_i^T \vec{\lambda},$$

$$\frac{\langle \phi \psi_j(\cdot; \vec{\lambda}) \rangle}{\langle \phi \rangle} \langle \mathbb{Q} \rangle \vec{\lambda} = \frac{\langle \phi \psi_j(\cdot; C_i^T \vec{\lambda}) \rangle}{\langle \phi \rangle} C_i \langle \mathbb{Q} \rangle C_i^T \vec{\lambda}.$$

Therefore, we conclude that for  $j \neq i$ ,  $\mathcal{D}^h(\vec{\lambda}) \vec{e}_j = C_i \mathcal{D}^h(C_i^T \vec{\lambda}) C_i^T \vec{e}_j$ , since  $C_i^T \vec{e}_j = \vec{e}_j$ . In the same way we can see that the conclusion holds for  $j = i$ , and therefore (4.4) follows. Finally, (4.5) follows by iterating (4.4) for  $i = 1, \dots, d$ .  $\square$

**5. Numerical simulations.** In this section, we present some numerical simulations of a two-dimensional aquifer using the effective parameters (hydraulic conductivity and macrodiffusivity) computed as in Sections 3 and 4. We compare the numerical simulations based on the macroscopic effective transport equations (3.26), (3.27), using the effective macrodiffusivity tensor given by (3.25), to the numerical simulations based on the local heterogeneous transport equations (2.3), (2.4). In the following we will call in short the numerical simulations of the effective transport equations (3.26), (3.27) *homogeneous simulations*, and the numerical simulations of the local heterogeneous transport equations (2.3), (2.4) will be called *heterogeneous simulations*. For both simplicity and less computational task we will consider a 2D heterogeneous aquifer, assuming symmetry of the heterogeneities and a diagonal hydraulic conductivity tensor. This last assumption will lead, by Proposition 4.4, to a symmetric effective macrodiffusivity tensor (3.25).

We perform the homogeneous simulation following the four steps:

1. Compute the effective hydraulic conductivity  $\mathbb{K}^h$ , by solving problems (3.3), and build the matrix  $\mathbb{Q}$  using (3.5);
2. Compute the effective Darcy's velocity  $\vec{q}^0$  by solving the problem (3.27);
3. For each  $x \in \Omega$  compute  $\mathbb{D}^h(x) = \mathcal{D}^h(\text{Pe}\nabla\overline{H}^0(x))$  by solving the problems (3.21) and using formula (3.22).
4. Perform the macroscopic concentration simulation by solving (3.26).

**5.1. Numerical methods.** Local problems (3.3) and (3.21) that have to be solved are linear and elliptic. To obtain an accurate approximation of (3.3) we can use either a mixed finite element method or a classical finite volume scheme to solve those problems and compute the effective hydraulic conductivity, as for example in [5]. But the local problems (3.21) are of convection-diffusion type, and then we prefer to use a finite volume scheme over uniform rectangular grids, with the convective term treated by full upwinding for the approximation of these problems. The finite volumes are then also used for problems (3.3).

The simulations were performed using an IMPES simulator which applies the mixed finite element method for computing hydraulic head and velocity and a finite volume method for the concentration equation. The same simulator is used for homogeneous and heterogeneous simulation. The code uses a suitable method for handling the full diffusivity tensors produced by the homogenization method. Only a short description of the method employed in this work will be given. The interested reader is referred to [21], [1] and [2] for more details.

The numerical methods feature the mixed finite element method over triangles as a solver to the Darcy flow equations (2.4) and (3.27). Our implementation uses a triangular mesh and the lowest order Raviart-Thomas elements i.e. a piecewise constant hydraulic head and a piecewise continuous flux (see, e.g., [16], [36]). Mixed methods provide a very accurate determination of the velocity field, but they also allow for a natural treatment of practical heterogeneous conditions. This method conserves mass in each cell and produces a direct approximation of the hydraulic head and the Darcy's velocity.

A conservative finite volume scheme is used for the concentration equations (2.3) and (3.26) (see [3] and [4]). The convective term is approximated with the aid of a Godunov scheme considered over the finite volume mesh dual to a triangular grid, whereas the diffusion term is discretized by piecewise linear conforming triangular finite elements. In the present case of vertex-centred finite volume, the secondary mesh is constructed by connecting element barycenters with edge midpoints. The

time discretization is explicit for the convection term and implicit for the diffusion part. This approach leads to a robust, conservative and stable scheme applicable for unstructured grids and the approximate solution has various interesting properties which correspond to the properties of the physical solution.

**5.2. Clustering of the Darcy velocity.** The approximation of the Darcy velocity field  $\vec{q}^0$  is constant by triangle since  $\text{div}\vec{q}^0 = 0$ , and therefore *d local problems* (3.21) should be solved for each triangle in the domain  $\Omega$ . From a practical point of view this is prohibitively expensive and unnecessary. In order to reduce the amount of the computations we use a kind of *clustering*. Namely, after the homogeneous Darcy's flow simulation is performed and all the Darcy velocity vectors  $\vec{q}_T^0$  are given in all triangles  $T$ , we group them into few classes or clusters. Then all vectors in the same cluster are "closed" and replaced by their mean value vector, say  $\vec{q}_{\text{mean}}^0$ . The tensor (3.22) is then calculated for  $\vec{\lambda} = \text{Pe}(\mathbb{K}^h)^{-1}\vec{q}_{\text{mean}}^0$  and applied to all triangles corresponding to the vectors in the cluster. We fix a priori the number of groups, or clusters, and this number will determine both the amount of calculations and the accuracy.

This clustering of vectors is performed in polar coordinates  $(r, \phi)$ , and we compute the rectangular domain  $(\phi_{\min}, \phi_{\max}) \times (r_{\min}, r_{\max})$  spanned by all Darcy's velocity vectors in the triangulation. We divide this rectangular domain uniformly into  $n \times m$  rectangles, each one representing one cluster (possibly empty) of vectors.

**5.3. Lagrangian effective diffusivity.** In order to compare the solutions of equation (2.3), denoted  $c^{\text{het}}$ , and the solutions of equation (3.26), denoted  $c^{\text{hom}}$ , for short times, we use the relative  $L^2$ -error:

$$l2err = \frac{\|c^{\text{het}}(\cdot, t) - c^{\text{hom}}(\cdot, t)\|_{L^2(\Omega)}}{\|c^{\text{het}}(\cdot, t)\|_{L^2(\Omega)}}. \quad (5.1)$$

The homogenization technique we used in this paper, and in [12], to derive the effective macrotransport equation (3.20) is based on an Eulerian formulation since the effective macrodiffusion is obtained by the averaged flux due to a given mean Darcy's velocity (see (3.21), (3.22) and (3.25)). An alternative approach consists in studying the motion of a single solute particle transported by the incompressible velocity field  $\vec{q}$  and diffused according to the diffusivity tensor  $\mathbb{D}$ , which **must be taken to be constant**. The equation of the motion of the solute particle, located at  $x = x_0$  and  $t = 0$ , is a stochastic differential equation of the form:

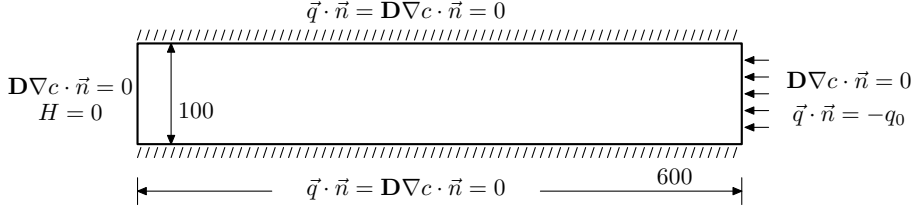
$$dX(t) = \vec{q}(X(t))dt + \mathbb{B}d\mathbf{W}(t), \quad (5.2)$$

where the matrix  $\mathbb{B}$  is given by  $\mathbb{D} = \frac{1}{2}\mathbb{B}\mathbb{B}^T$ , and  $\mathbf{W}(t)$  represents a  $d$ -dimensional Brownian motion. Using (5.2) the Lagrangian effective diffusivity is defined by:

$$(\mathbb{D}_L^h)_{i,j} = \lim_{t \rightarrow \infty} \frac{\phi}{2} \frac{d}{dt} [(\langle X(t) - \langle X(t) \rangle_W \rangle_W)_i (\langle X(t) - \langle X(t) \rangle_W \rangle_W)_j] \quad (5.3)$$

where  $\langle \cdot \rangle_W$  represents the expectation with respect to the Brownian motion, and the porosity is taken to be constant.

For a comparison of the long time behavior, as in the Lagrangian approach (see [7], [15]), we use the first three spatial moments for characterizing the effective transport

FIG. 6.1. The Domain  $\Omega$  and the boundary conditions for test problem 1.

model:

$$M_0(t) = \int_{\Omega} \phi(x)c(x,t) dx, \quad M_1^i(t) = \frac{1}{M_0(t)} \int_{\Omega} x_i \phi(x)c(x,t) dx, \quad (5.4)$$

$$M_2^{i,j}(t) = \frac{1}{M_0(t)} \int_{\Omega} (x_i - M_1^i(t))(x_j - M_1^j(t))\phi(x)c(x,t) dx, \quad (5.5)$$

for  $i, j = 1, 2$ . They will be calculated in both homogeneous and heterogeneous simulations and compared to each others.

It was shown in [26] that  $\mathbb{D}_L^h$  is then equal to the symmetric part of the Eulerian effective diffusivity  $\mathbb{D}^h$ , and moreover, that if  $c(x,t)$  is the transition probability density associated to (5.2) then  $(\mathbb{D}_L^h)_{i,j}$  can be written as:

$$(\mathbb{D}_L^h)_{i,j} = \lim_{t \rightarrow \infty} \frac{\phi}{2} \frac{d}{dt} M_2^{i,j}(t). \quad (5.6)$$

Therefore, in order to compare our results and to measure the quality of the upscaling procedure, we will choose the initial condition as a **sharp** Gauss pulse and we will then use the moments (5.4)–(5.5) and the estimates

$$d_{i,j}(t) = \frac{1}{2} \langle \phi \rangle \frac{d}{dt} M_2^{i,j}(t). \quad (5.7)$$

**REMARK 5.1.** All computations presented in Sections 6.2 and 6.3 have been performed with a dimensional form of the mesoscale and the macroscale equations. **TO BE REMOVED** In that form the Peclet number does not appear explicitly in (3.25).

## 6. Test results.

**6.1. Simulation data.** Inspired from an example, given in [6], of a pollutant spreading in an aquifer we consider a rectangular domain  $\Omega = (0, L_x) \times (0, L_y)$ , with  $L_x = 600$  m,  $L_y = 100$  m, that represents a vertical soil cross-section (Figure 6.1).

The domain is covered by a grid of  $40 \times 20$  rectangular cells  $(0, l_x) \times (0, l_y)$ , with  $l_x = 15$ ,  $l_y = 5$  (Figure 6.2). Each cell contains a symmetrically placed square inclusion like in Figure 6.2.

All physical properties have constant values in the matrix and in the inclusions. The porosity is  $\phi = 0.3$ ; and the hydraulic conductivity tensor (m/day) is:

$$\mathbb{K}_{\text{matrix}} = \begin{bmatrix} 1 & 0 \\ 0 & 0.1 \end{bmatrix}, \quad \mathbb{K}_{\text{inclusion}} = 10^{-4} \begin{bmatrix} 1 & 0 \\ 0 & 0.1 \end{bmatrix}.$$

The diffusivity tensor (m<sup>2</sup>/day) is given by:

$$\mathbb{D}_{\text{matrix}} = 10^{-2} \begin{bmatrix} 5 & 0 \\ 0 & 1 \end{bmatrix}, \quad \mathbb{D}_{\text{inclusion}} = 10^{-4} \begin{bmatrix} 5 & 0 \\ 0 & 5 \end{bmatrix}.$$

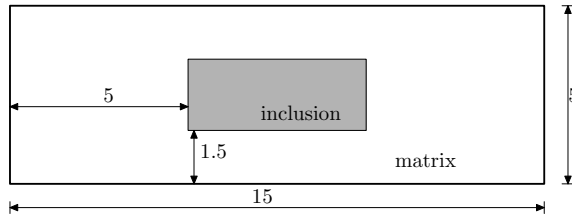


FIG. 6.2. Periodic rectangular cell.

Finally, we consider two different boundary conditions. In Section 6.2, we impose an unidirectional flux on the right side boundary, as shown in Figure 6.1, making the problem almost one-dimensional (this case will be used, essentially to measure the influence of the numerical diffusion in the two simulations). In Section 6.3, the inflow boundary will be a part of the upper boundary of the aquifer, as shown on Figure 6.7.

In order to measure the diffusion/dispersion by means of the first and the second moments (5.4), (5.5), we choose as initial condition the Gauss pulse ( $A = 5\pi$ ,  $\sigma^2 = 2.5$ ,  $(x_0, y_0) = (500, 85)$ ):

$$c(x, 0) = \frac{A}{2\pi\sigma^2} \exp\left(-\frac{1}{2\sigma^2}[(x - x_0)^2 + (y - y_0)^2]\right).$$

**6.2. The first test problem: unidirectional flow.** In this case we run three simulations with different Peclet numbers. Outcomes from heterogeneous and homogeneous simulations are compared through the function  $d_{1,1}(t)$ , given by (5.7). We compute the  $d_{1,1}(t)$  values obtained from heterogeneous and homogeneous simulations (denoted respectively  $d_{1,1}^{het}(t)$  and  $d_{1,1}^{hom}(t)$ ) and compare them to the effective macrodiffusivity  $\mathbb{D}_{1,1}^h$ , computed by (3.25). It is easy to see that for a flow with constant Darcy's velocity, constant porosity and diffusivity, the estimates  $d_{i,j}(t)$ , given by (5.7), are constant and equal to  $\mathbb{D}_{i,j}$  until the solvent starts leaving the domain. Therefore, we have  $d_{1,1}^{hom}(t) = \mathbb{D}_{1,1}^h$  until the solvent starts leaving the domain. We measure the convection–diffusion ratio by a local Peclet number which is:

$$\text{Pe} = \frac{|\langle q_x \rangle| l_x}{\langle \mathbb{D}_{1,1} \rangle},$$

where  $\langle \cdot \rangle$  is the mean value over  $\Omega$ . The Peclet numbers are generally different in the heterogeneous and homogeneous simulations (because of the difference in diffusivity and the effective macrodiffusivity), and for sufficiently fast convection, the Peclet number in the homogeneous simulation will be smaller than in the corresponding heterogeneous one. We will therefore refer to the Peclet number in homogeneous simulations (respectively in heterogeneous simulations) as the “homogeneous Peclet number” (respectively the “heterogeneous Peclet number”).

We perform three simulations with the three local “heterogeneous Peclet numbers”  $\text{Pe} = 1.728, 3.45$  and  $6.192$ , corresponding respectively to the “global heterogeneous Peclet numbers”  $69.12, 138$  and  $247.6$ . The three corresponding results are given in Figures 6.3, 6.4 and 6.5.

The difference between the effective macrodiffusivity  $\mathbb{D}_{1,1}^h$ , computed from (3.25), and the estimated  $d_{1,1}^{hom}(t)$  effective macrodiffusion in homogeneous simulations, computed from (5.7), are shown in Figures 6.3, 6.4 and 6.5. This difference is a consequence of the effect of numerical diffusion in the simulation. For this we start by

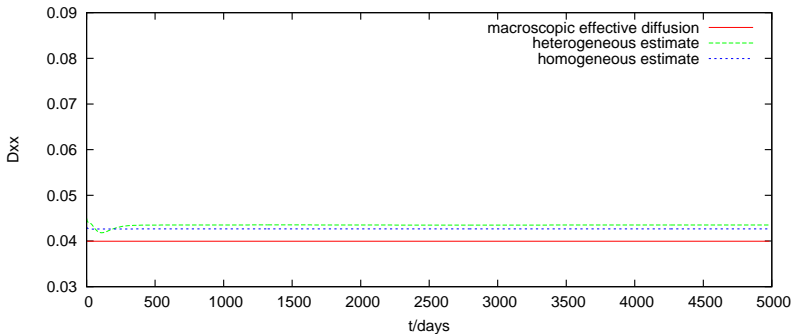


FIG. 6.3. Comparison of heterogeneous and homogeneous  $d_{1,1}(t)$  and  $\mathbb{D}_{1,1}^h$  for  $Pe = 1.728$ , in test problem 1.

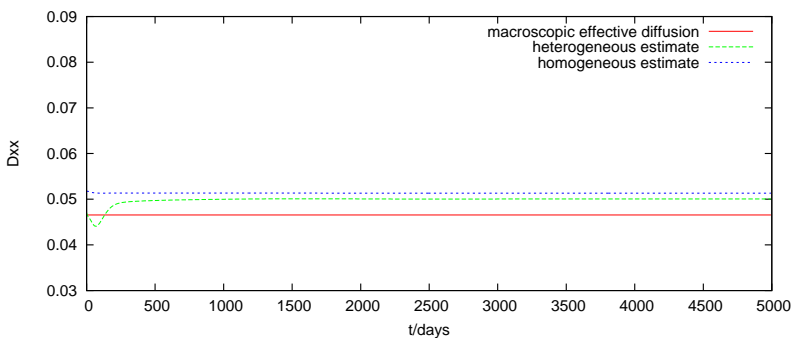


FIG. 6.4. Comparison of heterogeneous and homogeneous  $d_{1,1}(t)$  and  $\mathbb{D}_{1,1}^h$  for  $Pe = 3.45$ , in test problem 1.

quantifying the numerical diffusion in our first order scheme by roughly estimating it as in classical finite difference schemes by the *cell Peclet number*:

$$Pe_{\text{num}} = \frac{|\langle q_x \rangle| h}{2 \langle \mathbb{D}_{1,1} \rangle} = Pe \frac{h}{2l_x},$$

where  $h$  is the mesh size. In our example, having 89511 triangles in the domain we have  $h \approx 1.414$  and the three **cell Peclet numbers** are  $Pe_{\text{num}} \approx 0.079, 0.136$  and  $0.176$ . In all three figures the numerical diffusion is estimated by the difference between the effective macrodiffusivity  $\mathbb{D}_{1,1}^h$  and the estimated effective macrodiffusivity  $d_{1,1}^{hom}(t)$  in the homogeneous simulation. We verify, as postulated before, that the homogeneous cell Peclet number is a good estimate for the numerical diffusion: in Figure 6.3, 6.4 and 6.5 we have respectively 6.6%, 11.8% and 14.0% of numerical diffusion.

The results for the heterogeneous computations are rather different. **As in homogeneous simulation** there is an additional numerical diffusion (depending linearly on the Peclet number) which will lower artificially the importance of the mechanical dispersion, leading finally to underestimate the effective macrodiffusivity  $\mathbb{D}_{1,1}^h$ , by the estimate  $d_{1,1}^{het}(t)$  (as seen in Figure 6.5).

To understand this behaviour we first perform a simple test. We solve the cell

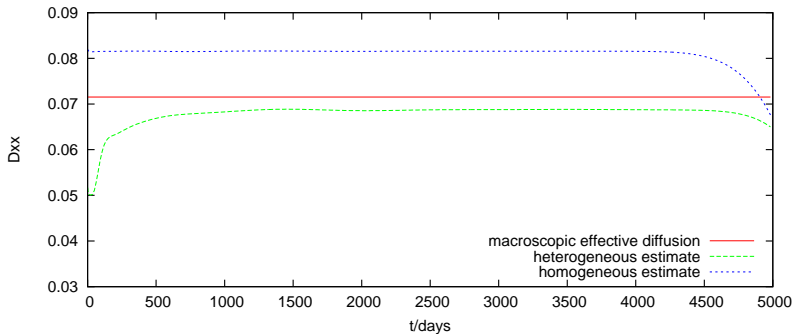


FIG. 6.5. Comparison of heterogeneous and homogeneous  $d_{1,1}(t)$  and  $\mathbb{D}_{1,1}^h$  for  $Pe = 6.192$ , in test problem 1.

problem (3.21) with  $\vec{\lambda} = v\vec{e}_1$ , for different values of the velocity  $v$  (in the range 0 to 1, corresponding to the local Peclet number in the range 0 to 330), in order to show the effective macrodiffusivity behavior for a given flow regime. In Figure 6.6 we see that the longitudinal effective macrodiffusivity  $\mathcal{D}_{11}^h(v\vec{e}_1)$ , calculated by (3.22), grows quadratically with  $v$  (that is with the Peclet number). In other words, in this example we are in a situation where the convection enhanced effective macrodiffusion is maximal (see [11], [22]). It was already observed in the literature (see for example [27]) that this maximal enhancement is due to the fact that the mean flow is parallel to one lattice axis, but when the flow is inclined to the lattice axis the longitudinal effective diffusivity may vary linearly with the velocity, which is the most often used assumption for natural media in the engineering literature.

Now we can conclude that the artificial lowering of the Peclet number by the presence of numerical diffusion in the simulation will lower “quadratically” the effect of mechanical dispersion. At higher Peclet numbers this effect cannot be compensated by the growth of the diffusivity, that is also a consequence of the presence of numerical diffusion, since it is linear with respect to the Peclet number. Therefore, we conclude that in these conditions the heterogeneous simulation shows less effective diffusivity than the exact solution.

**6.3. The second test problem: upper inflow.** In this example the Darcy’s velocity is no more constant and we will do a clustering of the computed Darcy’s velocity  $\vec{q}^0$  in order to reduce the amount of computation in the upscaling procedure, leading to the definition of a new velocity field  $\vec{q}^{app}$ , constant in each cluster and equal to the mean velocity in the cluster. In this example, we see that the error coming from the clustering process does not have a strong influence on the quality of the overall upscaling procedure. This is mostly due to the fact that the most rapid change in Darcy’s velocity field  $\vec{q}^0$  is localized around the point (400, 100), where we have a strong change in the velocity direction. More refined clustering will improve the effective macrodiffusivity tensor only locally, in the neighbourhood of that only point. For example, a clustering based on 33 different clusters gives a relative error in Darcy’s velocity of 12.76%, and a clustering with 80 different clusters will reduce the error down to only 8.28%. The error of the approximation is measured in the relative  $L^2$ -norm.

In Figure 6.8 we show the relative  $L^2$ -error of the concentration, defined in (5.1),

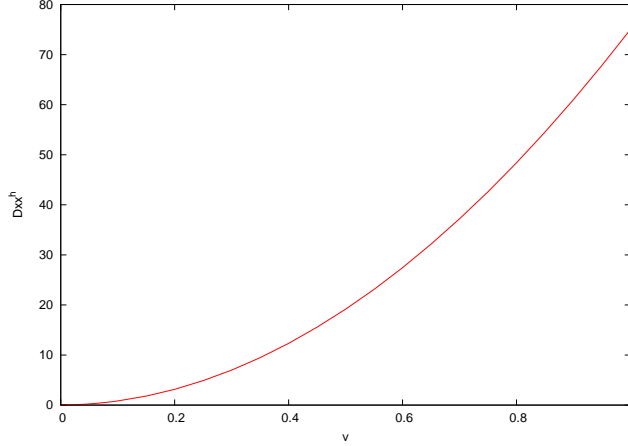


FIG. 6.6. Longitudinal effective macrodiffusivity  $\mathcal{D}_{11}^h(v\vec{e}_1)$  in test problem 1.

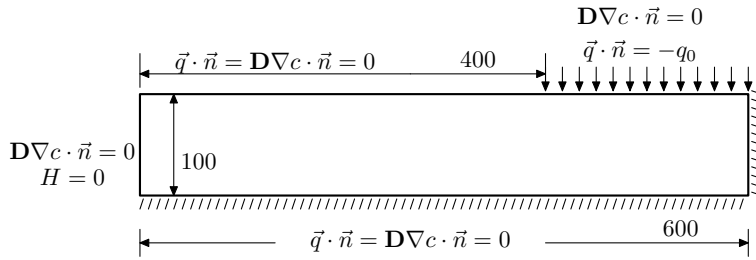


FIG. 6.7. The domain  $\Omega$  and the boundary conditions for test problem 2.

for the first 150 days, the time needed for the solution amplitude to drop to 5% of its initial value. Since the parameter  $\varepsilon = l_x/L_x = 0.025$ , we see that our  $L^2$ -error is of order  $\varepsilon$ , as predicted by the theory, according to the fact that the homogenized solution does not contain neither the oscillatory terms nor the boundary layer correctors.

In Figures 6.9, 6.10, 6.11 and 6.12, we consider the moments of order one and two as defined in (5.4), (5.5), according to [7] and [15], in order to compare the homogeneous simulations to the heterogeneous ones. We see in Figures 6.9 and 6.10 that the first order moments  $M_1^1(t)$  and  $M_1^2(t)$  in homogeneous and heterogeneous simulations are in good agreement, i.e. the Darcy velocity is well scaled up.

The difference in the computation of the second order moments, appearing in Figures 6.11 and 6.12, is a consequence, as explained in the first test problem, of the computed mechanical dispersion in heterogeneous simulation being lower than the enhancement of the macrodiffusion by convection (quadratically growing with the Peclet number) in formula (3.25). In the one hand there is additional numerical diffusion lowering the importance of the mechanical dispersion in the heterogeneous simulations, as explained before; in the other hand, for the homogeneous simulation, the mechanical dispersion is already included in the effective macrodiffusivity  $\mathbb{D}^h(x)$ , then the homogeneous Darcy's velocity is not oscillating, and therefore the numerical diffusion does not modify the already computed global dispersion. Having these effects in mind we may conclude that the second order moments are in good agreement with what we expected.



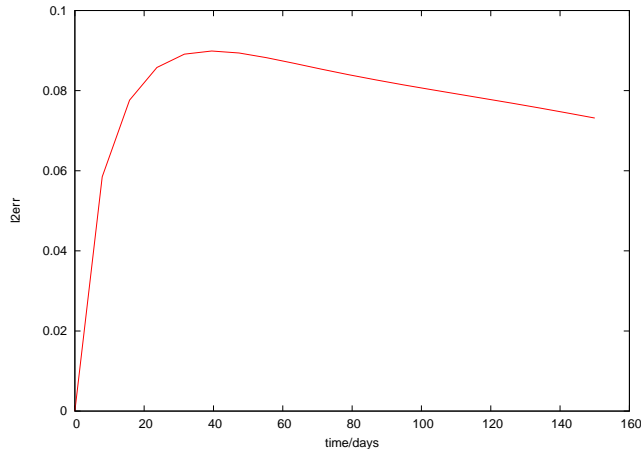


FIG. 6.8. The concentration relative  $L^2$ -error for test problem 2.

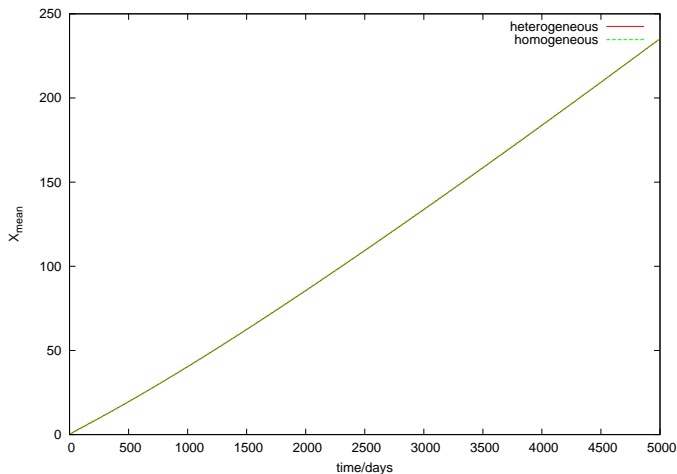


FIG. 6.9. Comparison of the first order moment  $M_1^1(t)$  in test problem 2, homogeneous vs. heterogeneous simulations.

In Figure 6.13 the dispersivity coefficients (see definition in [6]) in the longitudinal direction is shown as functions of time.

$$d_1 = \phi \frac{M_2^{1,1}(t)}{2M_1^1(t)}. \quad (6.1)$$

We verify for both simulations that this coefficient is not constant but is increasing with time (with traveled distance) which is consistent with the quadratic dependency on the Peclet number, and with the fact that the Peclet number grows slightly with the traveled distance.

Finally, we compare the level curves for the heterogeneous and homogeneous solute concentrations, given at  $t = 3889$  days, in Figures 6.14 and 6.15, respectively.

In conclusion, with the results of the simulations being carefully interpreted with respect to the numerical diffusion appearing in the computations, the simulations presented here show the good accuracy of the homogenization procedure for a **local**

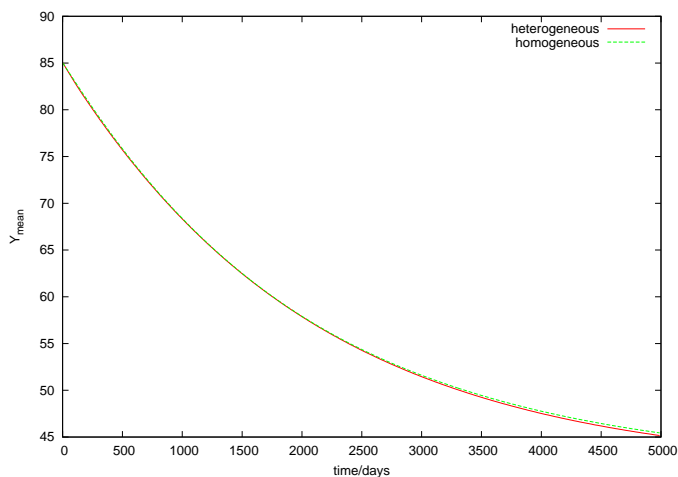


FIG. 6.10. Comparison of the first order moment  $M_1^2(t)$  in test problem 2, homogeneous vs. heterogeneous simulations.

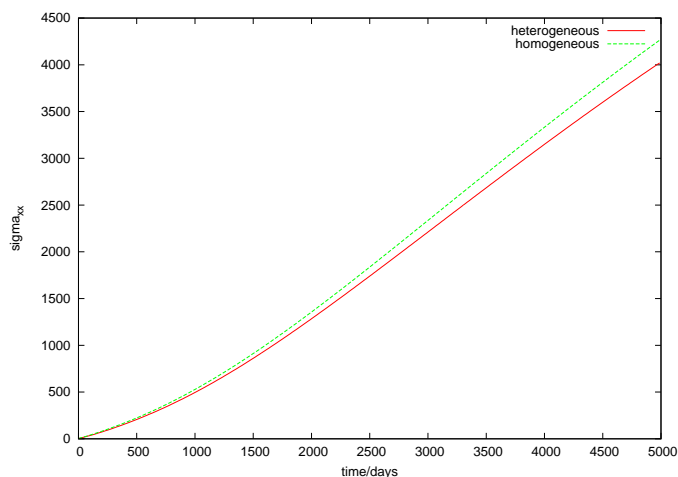


FIG. 6.11. Comparison of the second order moment  $M_2^{1,1}(t)$  in test problem 2, homogeneous vs. heterogeneous simulations.

**Peclet number of order 1.** Simulations with larger Peclet numbers would require higher order numerical method for convection-diffusion equation in order to avoid excessive numerical diffusion.

**Acknowledgements.** This work was supported partially from the GdR MoMaS CNRS-2439 ANDRA BRGM CEA EDF whose support is gratefully acknowledged. This paper was completed when M. Jurak was visiting the Applied Mathematics Laboratory of the University of Pau. He is grateful for the invitation.

#### REFERENCES

- [1] M. AFIF AND B. AMAZIANE, *Convergence of finite volume schemes for a degenerate convection-diffusion equation arising in flow in porous media*, Comput. Methods Appl. Mech. Engrg.,

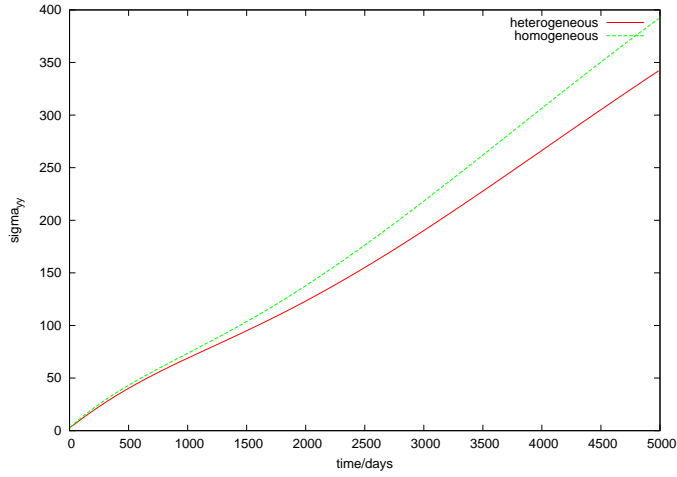


FIG. 6.12. Comparison of the second order moment  $M_2^{2,2}(t)$  in test problem 2, homogeneous vs. heterogeneous simulations.

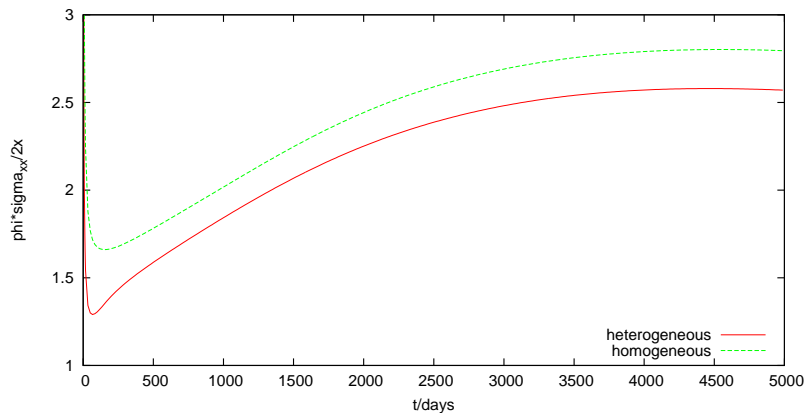


FIG. 6.13. Comparison of the dispersivity coefficient (6.1) in test problem 2, homogeneous vs. heterogeneous simulations.

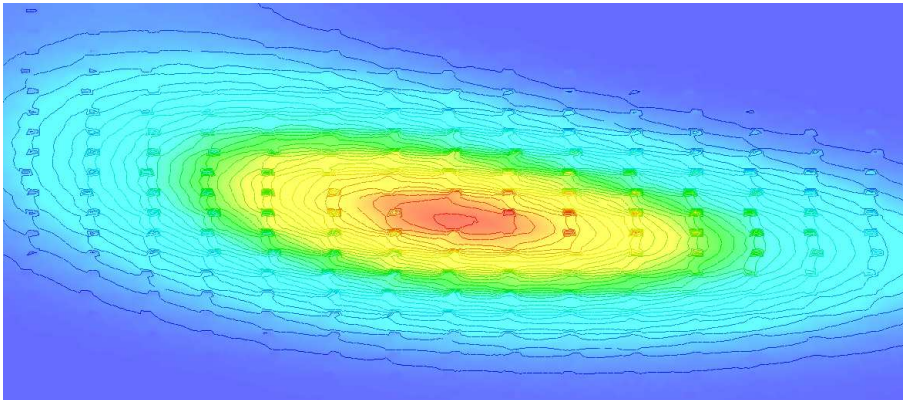


FIG. 6.14. Heterogeneous simulation:  $c(\cdot, t)$ ,  $t = 3889$  days, in test problem 2.

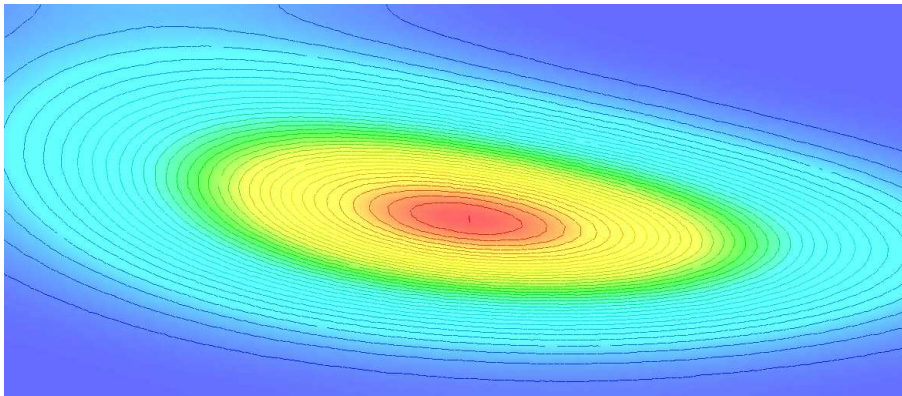


FIG. 6.15. Homogeneous simulation:  $c(\cdot, t)$ ,  $t = 3889$  days, in test problem 2.

- 191 (2002) pp. 5265–5286.
- [2] M. AFIF AND B. AMAZIANE, *Numerical simulation of two-phase flow through heterogeneous porous media*, Numerical Algorithms 34 (2003) pp. 117–125.
- [3] B. AMAZIANE, M. EL OSSMANI AND C. SERRES, *Numerical modeling of the flow and transport of radionuclides in heterogeneous porous media*, (2004), to appear. [http://lma.univ-pau.fr/data/pub/pub\\_pdf2004/0432.pdf](http://lma.univ-pau.fr/data/pub/pub_pdf2004/0432.pdf)
- [4] B. AMAZIANE AND M. EL OSSMANI, *Convergence analysis of an approximation to miscible fluid flows in porous media by combining mixed finite element and finite volume methods.*, (2005), to appear. [http://lma.univ-pau.fr/data/pub/pub\\_pdf2005/0505.pdf](http://lma.univ-pau.fr/data/pub/pub_pdf2005/0505.pdf)
- [5] B. AMAZIANE AND J. KOEBBE, *JHomogenizer: a computational tool for upscaling permeability for flow in heterogeneous porous media*, (2004), to appear. [http://lma.univ-pau.fr/data/pub/pub\\_pdf2004/0423.pdf](http://lma.univ-pau.fr/data/pub/pub_pdf2004/0423.pdf)
- [6] C. A. J. APPELO AND D. POSTMA, *Geochemistry, Groundwater and Pollution*, A. A. Balkema Publishers, Rotterdam, 1999.
- [7] R. ARIS, *On the dispersion of a solute in a fluid flowing through a tube*, Proc. Roy. Soc. London Series A, 235 (1956) pp. 67–77.
- [8] J.-L. AURIAULT AND L. LEWANDOWSKA, *Diffusion/adsorption/advection macrotransport in solids*, Eur. J. Mech., A/Solids, 15 (4) (1996) pp. 681–704.
- [9] A. AVELLANEDA AND A. J. MAJDA, *An integral representation and bounds of the effective diffusivity in passive advection by laminar and turbulent flows*, Commun. Math. Phys., 138 (1991) pp. 339–391.
- [10] J. BEAR, *Dynamics of Fluids in Porous Media*, Elsevier, Amsterdam, 1972.
- [11] R. N. BHATTACHARYA, V. K. GUPTA AND H. F. WALKER, *Asymptotics of solute dispersion in periodic porous media*, SIAM J. Appl. Math., 49 (1) (1989) pp. 86–98.
- [12] A. BOURGEAT, M. JURAK AND A. L. PIATNITSKI, *Averaging a transport equation with small diffusion and oscillating velocity*, Math. Meth. Appl. Sci., 26 (2003) pp. 95–117.
- [13] A. BOURGEAT AND M. KERN, Guest Editors, *Simulation of Transport around a Nuclear Waste Disposal Site: the Couplex Test Cases*, Computational Geosciences, Volume 8, Kluwer Academic Publishers, Netherlands, 2004.
- [14] A. BOURGEAT, A. MIKELIC AND S. WRIGHT, *Stochastic two-scale convergence in the mean and applications*, J. Reine Angew. Math., 456 (1994) pp. 19–51.
- [15] H. BRENNER AND D. A. EDWARDS, *Macrotransport Processes*, Butterworth-Heinemann, Stoneham, MA, 1993.
- [16] F. BREZZI AND M. FORTIN, *Mixed and Hybrid Finite Element Methods*, Springer-Verlag, New York, 1991.
- [17] Y. CAPDEBOSCQ, *Homogenization of a diffusion equation with drift*, C. R. Acad. S. Paris Sér. I Math. 327 (9) (1998) pp. 807–812.
- [18] Z. CHEN AND R. E. EWING, Editors, *Fluid Flow and Transport in Porous Media: Mathematical and Numerical Treatment*, American Mathematical Society, Providence, Rhode Island, 2002.
- [19] G. DAGAN, *Flow and Transport in Porous Formations*, Springer-Verlag, New York, 1989.
- [20] G. DE MARSILY, *Quantitative Hydrology*, Academic Press, London, 1986.

- [21] R. EYMARD, T. GALLOUET AND R. HERBIN, *The Finite Volume Method*, in Handbook of Numerical Analysis, P.G. Ciarlet and J.L. Lions, eds, North-Holland, Amsterdam, 2000, pp. 715–1022.
- [22] A. FANNJIANG AND G. PAPANICOLAOU, *Convection enhanced diffusion for periodic flows*, SIAM J. Appl. Math., 54 (2) (1994) pp. 333–408.
- [23] A. FANNJIANG AND G. PAPANICOLAOU, *Convection enhanced diffusion for random flows*, J. Statist. Phys., 88 (5-6) (1997) pp. 1033–1076.
- [24] V. K. GUPTA AND R. N. BHATTACHARYA, *Solute dispersion in multidimensional periodic saturated porous media*, Water Resour. Res., 22 (2) (1986) pp. 156–164.
- [25] V. V. JIKOV, S. M. KOZLOV AND O. A. OLEINIK, *Homogenization of Differential Operators and Integral Functionals*, Springer Verlag, Berlin, 1994.
- [26] D. L. KOCH AND J. F. BRADY, *The symmetry properties of the effective diffusivity tensor in anisotropic porous media*, Phys. Fluids, 30 (3) (1987) pp. 642–650.
- [27] C. K. LEE, C. C. SUN AND C. C. MEI, *Computation of permeability and dispersivities of solute or heat in periodic porous media*, Int. J. Heat Mass Transfer., 39 (4) (1996) pp. 661–676.
- [28] A. J. MAJDA AND P. R. KRAMER, *Simplified models for turbulent diffusion: Theory, numerical modelling, and physical phenomena*, Physics Reports, 314 (1999) pp. 237–574.
- [29] A. J. MAJDA AND R. M. MCLAUGHLIN, *The effect of mean flow on enhanced diffusivity in transport by incompressible periodic velocity fields*, Stud. Appl. Math., 89 (3) (1993) pp. 245–279.
- [30] R. MAURI, *Dispersion, convection, and reaction in porous media*, Phys. Fluids A, 3 (5) (1991) pp. 743–756.
- [31] D. W. MCLAUGHLIN, G. C. PAPANICOLAOU AND O. R. PIRONNEAU, *Convection of microstructure and related problems*, SIAM J. Appl. Math., 45 (5) (1985) pp. 780–797.
- [32] C. C. MEI, J.-L. AURIAULT AND CHIU-ON NG, *Some applications of the homogenization theory*, Advances in Applied Mechanics, 32 (1996) pp. 278–348.
- [33] M. PANFILOV, *Macroscale Models of Flow Through Highly Heterogeneous Porous Media*, Kluwer Academic Publishers, Dordrecht–Boston–London, 2000.
- [34] G. C. PAPANICOLAOU AND S. R. S. VARADHAN, *Boundary value problems with rapidly oscillating random coefficients*, in Colloquia Mathematica Societatis Janos Bolyai, 27 (1979) pp. 835–873.
- [35] O. A. PLUMB AND S. WHITAKER, *Dispersion in heterogeneous porous media*, Water Resources Research, 24 (7) (1998) pp. 913–938.
- [36] J. E. ROBERTS AND J.M. THOMAS, *Mixed and hybrid methods*, in Handbook of Numerical Analysis, P.G. Ciarlet and J.L. Lions, eds, North-Holland, Amsterdam, 2000, pp. 523–639.
- [37] P. ROYER, J.-L. AURIAULT, J. LEWANDOWSKA AND C. SERRES, *Continuum modelling of contaminant transport in fractured porous media*, Transport in Porous Media, 49 (2002) pp. 333–359.
- [38] J. RUBINSTEIN AND R. MAURI, *Dispersion and convection in periodic media*, SIAM J. Appl. Math., 46 (6) (1986) pp. 1018–1023.
- [39] G. TAYLOR, *Dispersion of soluble matter in solvent flowing slowly through a tube*, Proc. Roy. Soc. London Series A, 219 (1953) pp. 186–203.